SCIENTIFIC PAPERS

Shock wave diffraction and reflection around a dusty square cavity*

WANG Boyi (王柏懿), WANG Chao (王 超) and QI Longxi (戚隆溪)

Institute of Mechanics, Chinese Academy of Sciences, Beijing 100080, China

Received May 11, 2000; revised June 26, 2000

Abstract The diffraction and reflection of planar shock wave around a dusty square cavity is investigated numerically, which is embedded in the flat bottom surface of a two-dimensional channel, and the induced gas-particle two-phase flow. The wave patterns at different times are obtained for three different values of the particle diameter. The computational results show that the existence of particles affects appreciably the shock wave diffraction and cavity flow.

Keywords: shock wave, diffraction, reflection, dusty gas, cavity flow.

The investigation of interactions between dusty shock waves and rigid boundaries has attracted much attention in various engineering applications since the 1950s. Among them, public and industrial safety engineering is an important example. After an explosion, the effect of generated air blasts can travel quite a long distance via shock wave propagation and it is complicated due to the interaction between shock wave and structure-boundary. In many real situations, vast amounts of suspended fine particles exist in the atmosphere of accident scene, which is known as the dusty gas. With respect to shock propagation characteristics, there are appreciable differences between the pure gas case and the dusty gas case. Hence, the structure loading histories depend not only on the strength of incident shock wave and the structure geometry but also on the particle properties and the mass loading ratio of particles. Shock wave diffraction around a square cavity filled with the pure gas was studied by Igra et al.[1]. However, a cavity filled with the dusty gas represents an important real case, and it requires extending the study of single-phase flows to that of two-phase flows. The authors have considered the changes of shock wave patterns in baffle and nozzle systems due to the presence of suspended particles[2,3]. As another model problem, planar shock wave diffraction around a dusty square cavity, embedded in the flat bottom surface of a two-dimensional channel, is numerically studied in the present work. In this structure (Fig. 1), there are the pure air in the straight duct over the flat surface and the dusty gas inside the cavity. The incident planar shock wave with Mach number M_s propagates from left to right. In region I, ahead of the incident shock wave, air is quiescent and two-phase flow field is induced in region II,

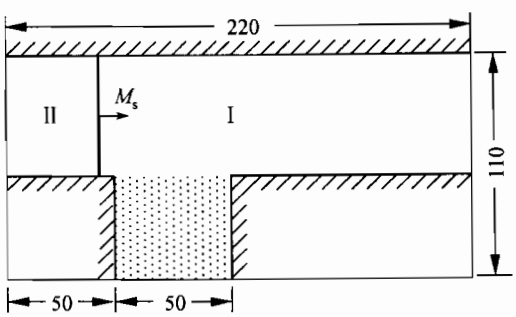

Fig. 1 Schematic of the flow field and computation domain (unit: mm).

* Project supported by the National Natural Science Foundation of China (Grant No. 19972069).

behind the incident shock wave. As is well known, the shock-induced flow is controlled by the interaction between the shock waves and cavity walls, which results in diffracted waves, reflected waves and shear layer or vortex. Moreover, secondary shock waves and expansion fans may be generated in the induced flow field. The effect of the presence of particles should be considered in all the mechanisms mentioned above.

1 Theory

At present, there are two theoretical models to simulate gas-particle flows: particle trajectory model and continuous medium model. In the particle trajectory model, one needs track each particle in the flow field and the computation work is very heavy for a system having a great number of particles (especially when particles possess different physical properties). Therefore, the two-fluid model is applied to the gas-particle suspension in this study: both the carrier phase (air) and the dispersed phase (particles) are treated as continuous media. The usual fluid equations are adopted except the terms for the gas-particle interaction. This paper deals with the dilute gas-particle mixture and assumes that air is a perfect gas and the volume fraction and the partial pressure of particles are negligible. The exchanges of momentum and energy take place on the particle surface, involving viscous force and thermal transfer.

For generality, all the independent variables (space coordinates x^*, y^* and time t^*) and flow parameters (density ρ^*, velocity components u^* and v^*, pressure p^*) are normalized to corresponding values in the pre-shock region I (denoted by subscript 1):

$$x = \frac{x^*}{l},\ y = \frac{y^*}{l},\ t = \frac{a_1 t^*}{l},\ \rho = \frac{\rho^*}{\rho_1},\ u = \frac{u^*}{a_1},\ v = \frac{v^*}{a_1},\ p = \frac{p^*}{\gamma p_1},$$

where $l = 8m/\pi\rho_{g1}d^2$ is the characteristic length (m and d are the particle mass and diameter respectively); $a_1 = \sqrt{\gamma p_{g1}/\rho_{g1}}$ the sound speed and γ the gas specific heat ratio. Then the nondimensional Euler equations can be written as

$$\frac{\partial U}{\partial t} + \frac{\partial F}{\partial x} + \frac{\partial G}{\partial y} = H, \tag{1}$$

where

$$U = \left[\rho_g, \rho_g u_g, \rho_g v_g, \left(\frac{\rho_g}{2}(u_g^2 + v_g^2) + \frac{p}{\gamma - 1}\right), \rho_p, \rho_p u_p, \rho_p v_p, \rho_p T_p\right]^T,$$

$$F = \left[\rho_g u_g, (\rho_g u_g^2 + p), \rho_g u_g v_g, u_g\left(\frac{\rho_g}{2}(u_g^2 + v_g^2) + \frac{\gamma p}{\gamma - 1}\right), \rho_p u_p, \rho_p u_p^2, \rho_p u_p v_p, \rho_p u_p T_p\right]^T,$$

$$G = \left[\rho_g v_g, \rho_g u_g v_g, (\rho_g v_g^2 + p), v_g\left(\frac{\rho_g}{2}(u_g^2 + v_g^2) + \frac{\gamma p}{\gamma - 1}\right), \rho_p v_p, \rho_p u_p v_p, \rho_p v_p^2, \rho_p v_p, T_p\right]^T,$$

$$H = \left[0, -\alpha\rho_p F_x, -\alpha\rho_p F_y, -\alpha\rho_p\left(u_p F_x + v_p F_y + \frac{\beta Q}{\gamma(\gamma - 1)}\right), 0, \rho_p F_x, \rho_p F_y, \rho_p Q\right]^T.$$

Here the subscripts g and p refer to the flow quantities of the gas and particle phases respectively; $\alpha = \rho_{p1}/\rho_{g1}$ is the mass loading ratio of particles and $\beta = C_m/C_v$ the ratio of specific heats of the two phases. In addition, for the interaction between gas and particles due to drag force F and heat transfer Q, the following empirical expressions of Ranz-Marschall equations are used[4,5]:

$$F_x = \rho_g(u_g - u_p)\sqrt{(u_g - u_p)^2 + (v_g - v_p)^2}(0.48 + 28Re^{-0.85}); \tag{2}$$

$$F_y = \rho_g(v_g - v_p)\sqrt{(u_g - u_p)^2 + (v_g - v_p)^2}(0.48 + 28Re^{-0.85}); \tag{3}$$

$$Q = \frac{8\mu_1\gamma}{d\beta a_1\rho_{g1}\mathrm{Pr}}\left(\frac{T_g}{T_{g1}}\right)^{0.768}(T_g - T_p)(2.0 + 0.6Pr^{1/3}Re^{1/2}); \tag{4}$$

where $Re = \rho_g|v_g - v_p|d/\mu$ is the slip Reynolds number based on the particle diameter, Pr the Prandtl number and μ_1 the viscosity of air in region I ahead of the incident shock wave.

By using the operator-splitting procedure, Eq. (1) is split into three equations:

$$\frac{\partial U}{\partial t} + \frac{\partial F}{\partial x} = 0, \tag{5}$$

$$\frac{\partial U}{\partial t} + \frac{\partial G}{\partial y} = 0, \tag{6}$$

$$\frac{\mathrm{d}U}{\mathrm{d}t} = H. \tag{7}$$

Obviously, in Eqs. (5) and (6) there are no coupling between the gas and particle phases. Therefore, the gas-phase equation and particle-phase equation can be solved independently using general riemann problem (GRP) scheme[6] and MacCormack scheme[7]. Eq. (7) includes the phase-interaction terms and can be solved by the predictor-corrector method. Let L_x and L_y denote the operators of GRP or MacCormack schemes corresponding to Eqs. (5) and (6), L_r the operator of predictor-corrector scheme corresponding to Eq. (7). According to Strang's principle of operator symmetry[8],

$$U_{i,j}^{n+1} = L_r\left(\frac{\Delta t}{2}\right)L_x\left(\frac{\Delta t}{2}\right)L_y(\Delta t)L_x\left(\frac{\Delta t}{2}\right)L_r\left(\frac{\Delta t}{2}\right)U_{i,j}^{n}. \tag{8}$$

It can be seen that Eq. (8) is a second-order finite-difference approximation to Eq. (1).

2 Results

The numerical simulations of shock-induced flow field were completed for six cases where the Mach number of incident shock wave $M_s = 1.30$ and 2.032 and the particle diameter $d = 1$, 10 and 50 μm. In all the six cases, the following three parameters took the same values: the particle mass loading ratio $\alpha = 1$, the ratio of specific heats of the two phases $\beta = 1$ and the particle material density $\sigma_p = 2500$ kg/m^3. In order to show the effects of particle existence, the pure gas case was also considered in the calculations.

For the case $M_s = 1.30$, the flows behind the incident shock wave are subsonic. Fig. 2 plots the density contours for the pure gas case and dust gas case, where $d = 10$ μm for the latter case. It shows the evolution of the various waves at different times when the incident shock wave propagates across the cavity. When $t = 180$ μs (Fig. 2(a)), the incident shock wave moves over the cavity with a reflected shock and a diffracted shock in the cavity, while a vortex appears on the upper-left corner. When $t = 200$ μs (Fig. 2(b)), the diffracted shock arrives to the downright corner and disappears. At that moment, there are only two reflected shocks in the cavity. When $t = 240$ μs (Fig. 2(c)), there occur intersection of the reflected shocks and interaction between the reflected shock and the vortex. As a result the cavity flow becomes quite complicated. Compared with the pure gas case, particles do not affect the transmitted shock wave in the duct, but they appreciably influence the diffracted and reflected shock waves in the cavity. In other words, due to the presence of particles, the diffracted and reflected shock waves are dissipated: shock speed is slower and shock strength is smaller.

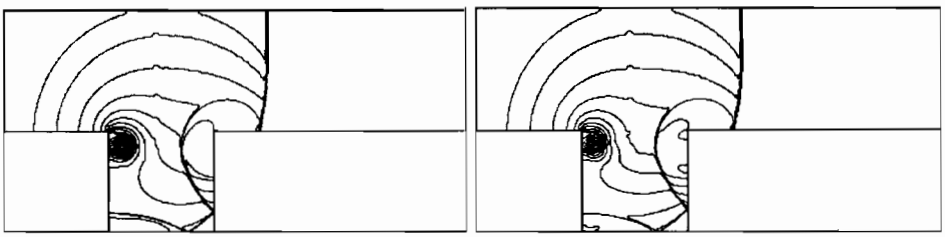

(a) t =180 μs

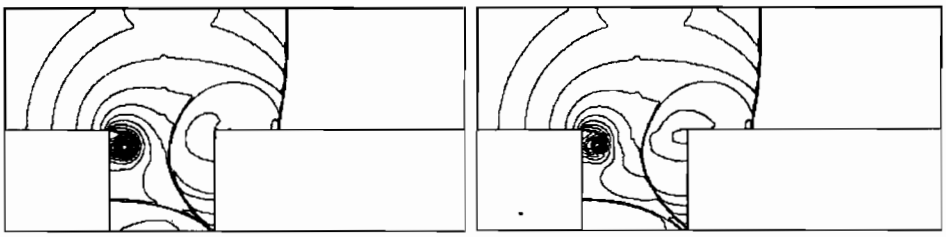

(b) t =200 μs

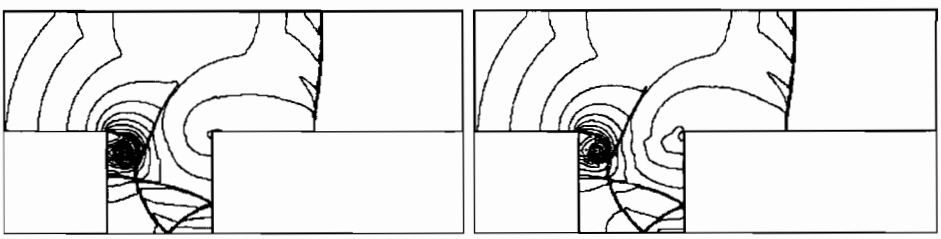

(c) t =240 μs

Fig. 2 Isopyknics when $M_s = 1.30$ and $d = 10$ μm ($\Delta\rho/\rho = 0.05$). Left column: pure gas case; right column: dusty gas case.

Figure 3 shows the effect of particle size on cavity flows where the incident shock Mach number keeps constant ($M_s = 1.30$). Two different diameters were chosen ($d = 1$ μm and 50 μm) and the

time was fixed at $t = 200\ \mu s$. Fig. 3(a) shows that the shock waves in the cavity disperse to compressible waves in the cavity when the particle diameter is small enough. Fig. 3(b) shows that all shock waves in the cavity change little when the particle diameter is large enough.

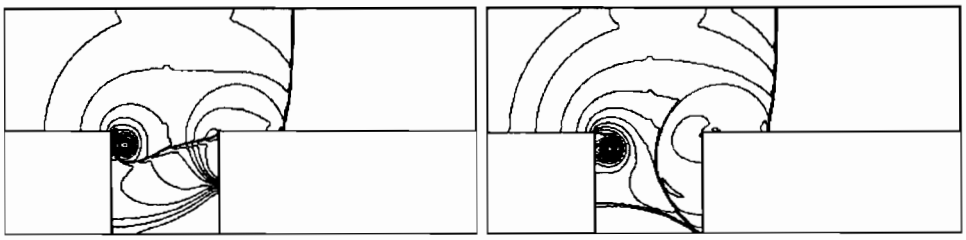

Fig. 3 Isopycnics when $M_s = 1.30$ and $t = 200\ \mu s$ ($\Delta\rho/\rho = 0.05$). Left: particle diameter $d = 1\ \mu m$; right: particle diameter $d = 50\ \mu m$.

For the case $M_s = 2.032$, supersonic flows occur behind the incident shock wave. Fig. 4 plots the density contours for the pure gas case and the dusty gas case (for the latter case the particle diam-

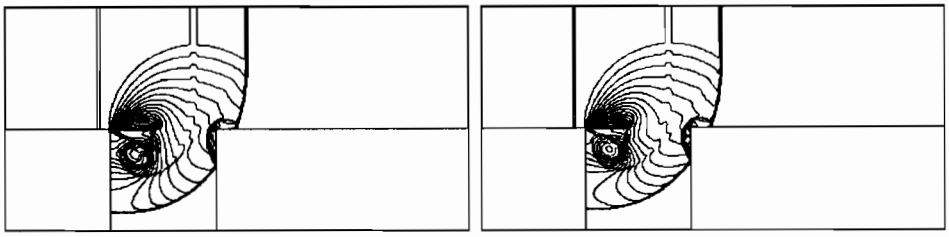

(a) $t = 100\ \mu s$

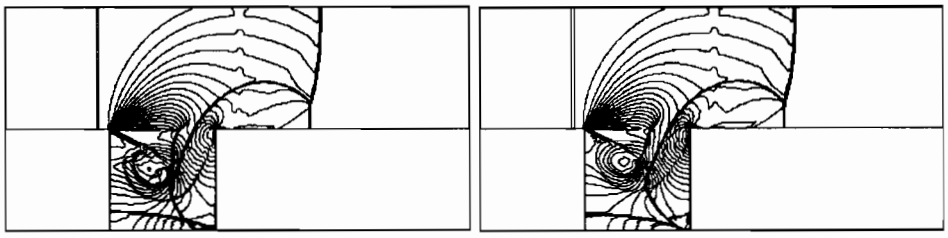

(b) $t = 150\ \mu s$

(c) $t = 250\ \mu s$

Fig. 4 Isopycnics when $M_s = 2.032$ and $d = 10\ \mu m$ ($\Delta\rho/\rho = 0.1$). Left column: pure gas case; right column: dusty gas case.

eter d = 10 μm), at the time t = 100, 150 and 250 μs. Under this condition, a secondary shock wave is clearlyvisible in the gas phase density contours. Obviously, the flow fields inside the cavity is more complicated becausethere are the interactions of secondary shock wave and reflected shock wave, as well as secondary shock wave and vortex, etc. Compared with the pure gas case or the low Mach numbercase, particles have stronger effect on the diffracted and reflected shock waves.

The results corresponding to the incident shock wave $M_s = 2.032$, for the particle diameter d = 1 μm and 50 μm, at t = 150 μs are given in Fig. 5. As in to the low Mach number case, the effect of particle size on the diffracted and reflected shock waves is stronger for smaller particle size when the particle mass loading ratio is the same.

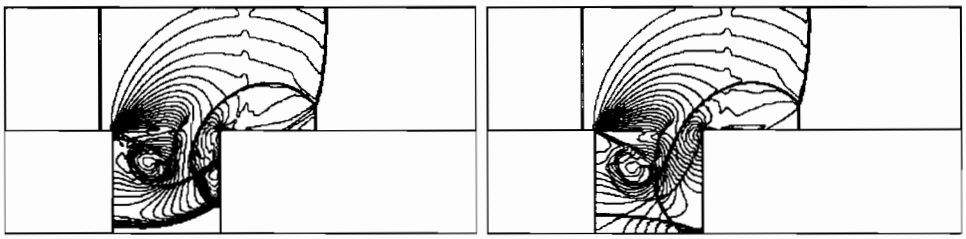

Fig. 5 Isopycnics when $M_s = 2.032$ and t = 150 μs ($\Delta\rho/\rho = 0.1$). Left: particle diameter d = 1 μm; right: particle diameter d = 50 μm.

3 Conclusions

The computations show clearly the entire shock wave diffraction process as the time escapes: expansive diffraction, collision reflection, vortex shedding and secondary shock compression. These numerical simulations of wave patterns indicate. (i) The incident shock wave starts diffraction and shedding of vortex when it reaches the cavity upper-left corner. (ii) The incident shock wave splits into transmitted and reflected shock waves when it hits the cavity upper-right corner. (iii) When the flow behind the incident shock wave is supersonic, there are expansive fans at the upper-left corner of cavity and a secondary shock wave in the cavity.

With respect to the effect of particle presence, the obtained results show that the particles have an appreciable influence on the cavity flow, as compared to the corresponding pure-gas cases. As the particle size decreases, the shock wave moves slower and the interaction between gas and particles becomes stronger. When the particle diameter is small enough, the dusty shock wave would be dispersed.

References

1 Igra, O. et al. Experimental and numerical study of the interaction between a planar shock wave and a square cavity. J. Fluid Mech, 1996, 313: 105.

2 Wang, B. Y. et al. Shock-induced two-phase flows in an aligned baffle system filled with suspended particles. Shock Waves, 1996, 6: 367.

3 Wu, Q. S. et al. Wave pattern characteristics of a two-phase nozzle flow by shock propagation. Shock Waves, 1997, 7: 127.

4 Gilbert, M., et al. Velocity lag of particle in linearly accelerated combustion gases, Jet Prop., 1995, 25: 26.
5 Knudsen, J. G. et al. Fluid Mechanics and Heat Transfer, New York: McGraw-Hill, 1958.
6 Ben-Artzi, M. et a. A second-order Godunov-type scheme for compressible fluid dynamics. J Comput Phys. 1984, 55:1.
7 MacCormack, R. W. The effect of viscosity on hypervelocity impact cratering. AIAA-69-354, 1969.
8 Strang, G., On the construction and comparison of difference schemes. SIAM J. Numer. Anal., 1968, 5: 506.